Pergamon

Spill Science & Technology Bulletin, Vol. 7, Nos. 5–6, pp. 279–288, 2002

Printed in Great Britain
1353-2561/02 $ - see front matter

PII: S1353-2561(02)00075-0

RESEARCH

Drift Modeling of Cargo Containers

PIERRE DANIEL†*, GWÉNAËLE JAN‡, FANCH CABIOC'H§, YVES LANDAU† & ERWANN LOISEAU†
†*Météo-France, DPrévi/MAR, 42 Avenue Coriolis, 31057 Toulouse Cedex, France*
‡*LODYC Lab., University of Paris VI, 4 Place Jussieu, 75252 Paris Cedex 05, France*
§*Cedre, Rue Alain Colas, BP 20413, 29604 Brest Cedex, France*

Containers lost at sea are a hazard for shipping. The maritime authorities thus wish to be able to announce their positions to the navigators, or to recover them. In the event of containers loss, the calculation of the trajectory enables to locate the dangerous area for navigation and to search for the containers. A numerical model has been developed and configured to provide a tool to forecast container drift at the sea. This paper summarises the key features of the model and presents four simulations in hindcast mode. Three cases are real losses ('Churruca', 'Sherbro' and tank containers), one is an experiment (Dourvarc'h).

A basic physic of the container has been implemented in the hydrodynamic code developed by Météo-France. This aspect constitutes a new approach in the prediction of objects drifting on the sea. We demonstrate by the analytical calculus and with the four studied cases that the immersed fraction initialised in the initial condition is a key parameter. The results have also shown the role of the wind direction and intensity on the trajectories simulations and the sensitivity of the model to the container buoyancy term.

Keywords: **Ocean circulation modeling, shipping, cargo containers' drift projection, navigation hazzards, marine debris, pollution**

Introduction

General use containers are standardised at the international level and there are two types of containers: 20 feet length (6.058 × 2.438 × 2.438 m) and 40 feet length (12.192 × 2.438 × 2.438 m). In the model, we assume that containers are flat in the water and they align with the wind. However, there are cases where the ballast inside the container can shift. Shifting of the ballast leads to one corner or side sinking lower in the water than it opposite side or diagonal corner. General-use containers are not water-proof in water. They are more likely to ship water if they have been damaged during a fall from a vessel deck to the ocean surface. In most cases, empty containers sink within 30 min. In the model, we consider containers which do not sink. Their immersion is variable. It may remain constant or be a function of time.

Another type of container can be found: tank-container. This type of container is intended for the transport of liquid or gas. It consists of two basic elements: the tank and the framework which is an open rectangular box standard to shipping containers (20 × 8 × 8 ft). Empty tank-containers do not sink their immersion is also variable.

Model Description

The model equations are similar to the equations describing iceberg motion such as in Crépon *et al.* (1988), Smith (1993), Bigg *et al.* (1996) or Perrie and Hu (1997) models. The basic physics of the container has been implemented in the hydrodynamic code developed by Météo-France. The physics of the container takes into account the wind action on the emerged surface.

*Corresponding author. Tel.: +33-561-07-82-09; fax: +33-561-07-82-92.
E-mail address: pierre.daniel@meteo.fr (P. Daniel).

Hydrodynamic model: basic equations

The water velocity is provided by a coupling between a 2D hydrodynamic limited area ocean model and a 1D eddy viscosity model (Daniel, 1996, 1998). The objective of this approach is to enable a realistic representation of near-surface current velocity structure.

The 2D hydrodynamic, limited area, ocean model solves the non-linear shallow water equations on a fixed grid mesh:

$$\frac{\partial \vec{q}}{\partial t} + \vec{q}\nabla\vec{q} + f\vec{k}\Lambda\vec{q} = -g\vec{\nabla}\eta - \frac{1}{\rho}\vec{\nabla}P_a + \frac{1}{\rho H} \times (\vec{\tau}_s - \vec{\tau}_b) + A\nabla^2\vec{q} \quad (1)$$

$$\frac{\partial \eta}{\partial t} + \nabla(H\vec{q}) = 0$$

where t denotes time, q the depth-integrated current, η the sea surface elevation, H the total water depth, f the Coriolis parameter, k a unit vector in the vertical, P_a the atmospheric surface pressure, τ_s the surface wind stress, τ_b the bottom frictional stress, ρ the density of water, g the gravitational acceleration, A the horizontal diffusion coefficient (2000 m^2/s).

These equations, written in spherical polar coordinates, are integrated forward in time on an Arakawa C-grid using a split-explicit finite difference scheme.

Boundary conditions at the sea surface. The surface wind stress components are computed using the quadratic relationship:

$$\begin{cases} \tau_{sx} = \rho_a C_d |V_a| V_{ax} \\ \tau_{sy} = \rho_a C_d |V_a| V_{ay} \end{cases} \quad (2)$$

V_{ax}, V_{ay} are the horizontal components of wind velocity 10 m above the sea surface, ρ_a is the air density and C_d is the drag coefficient calculated by the Wu formulation:

$$C_d = (0.8 + 0.065|V_a|)10^{-3}$$

(Wu, 1982, coefficient without dimension).

Boundary conditions at the sea bottom. The bottom topography was hand extracted from nautical charts on a 5-min grid mesh. The bottom stress is computed from the depth-integrated current using a quadratic relationship. The bottom stress components are computed using the quadratic relationship:

$$\begin{cases} \tau_{bx} = \rho_w C_b |q| q_x \\ \tau_{by} = \rho_w C_b |q| q_y \end{cases} \quad (3)$$

q_x, q_y are the horizontal components of depth integrated current, ρ_w is the water density and C_b, the drag coefficient is fixed to 0.002.

Horizontal boundary conditions. At coastal boundaries the normal component of velocity is set to zero. At open boundaries, the sea surface elevation is given by the tide and the inverted barometer effect. A gravity wave radiation condition is used for the current.

Vertical profile of the current

The shear current is calculated analytically with a bilinear eddy viscosity model that assumes the vertical eddy viscosity to increase linearly with the distance from both the water surface and the bottom boundary (Poon & Madsen, 1991). The governing equation is

$$\frac{\partial \hat{U}}{\partial t} + \mathrm{i}f\hat{U} = -\frac{1}{\rho}\frac{\partial P}{\partial n} + \frac{\partial}{\partial z}\left(\nu_t \frac{\partial \hat{U}}{\partial z}\right) \quad (4)$$

$\hat{U} = u + \mathrm{i}v$ is the complex horizontal velocity (u and v are the components of current), ν_t is an eddy viscosity and $(\partial/\partial n) = (\partial/\partial x) + \mathrm{i}(\partial/\partial y)$.

We employ a bilinear viscosity model proposed by Madsen (1977):

$$\begin{cases} \nu_t = -K u_{*s} z & \text{if } -Z_m < z \leqslant 0 \\ \nu_t = K u_{*b}(z + h) & \text{if } -h \leqslant z \leqslant -Z_m \end{cases} \quad (5)$$

h is the ocean depth, $K = 0.4$ is the Von Karman constant, u_{*s} and u_{*b} are the shear velocities, defined by the surface and bottom shear stresses, respectively, and

$$z_m = \frac{h u_{*s}}{u_{*s} + u_{*b}} \quad (6)$$

The viscosity model is coupled to the ocean model by:

$$q = \frac{1}{h}\int_0^h U \, \mathrm{d}z \quad (7)$$

Container model

The basic movement conservation equation is:

$$m\frac{\partial \vec{V}}{\partial t} + mf\vec{k}\Lambda\vec{V} = \vec{F}_a + \vec{F}_w + \vec{F}_r \quad (8)$$

t denotes time, m the mass of the container, V the horizontal velocity, f the Coriolis parameter, k a unit vector in the vertical, F_a the wind drag and F_w the water drag, F_r the wave radiation force (Fig. 1).

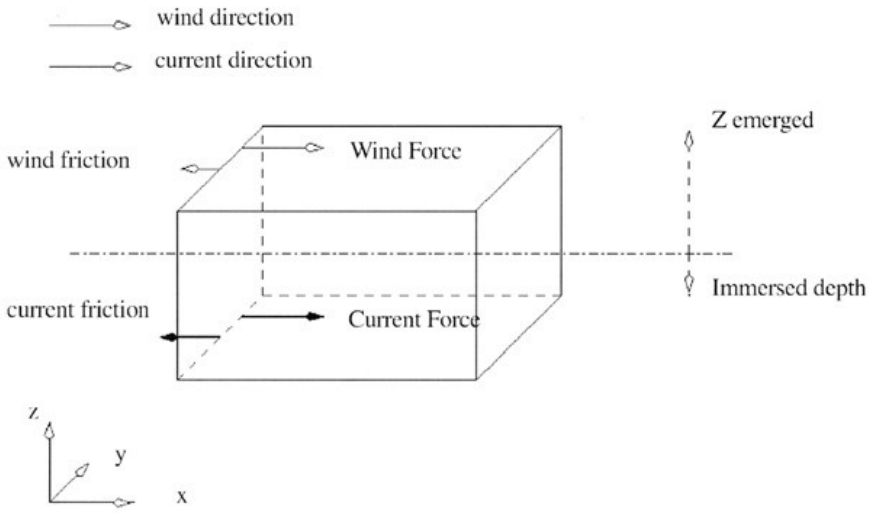

Fig. 1 Drift forces and parameters.

The wind drag is:

$$\vec{F}_a = \frac{1}{2}\rho_a C_a S_a |\vec{V}_a - \vec{V}|(\vec{V}_a - \vec{V}) \tag{9}$$

ρ_a is the air density, C_a is the drag coefficient, S_a is the cross-sectional area affected by the wind and V_a is the wind velocity at 10 m, available in the atmospheric analysis data sets.

Air drag coefficient of bluff objects at high Reynolds number is typically about 1 (Smith, 1993), so an a priori value of 1.0 is chosen for C_a.

For the immersed section, the water drag is:

$$\vec{F}_w = \frac{1}{2}\rho_w C_w S_w |\vec{V}_w - \vec{V}|(\vec{V}_w - \vec{V}) \tag{10}$$

where ρ_w is the water density, C_w is a drag coefficient, S_w is the cross sectional area affected by the water and V_w is the water velocity.

Experimental work (Cabioc'h & Aoustin, 1997) gives $0.8 < C_w < 1.2$; in the present work, we use $C_w = 1.0$

We neglect tangential drag force for both air and water drag since it is respectively 500 and 50 times lower than the normal drag force (Crépon *et al.*, 1988).

The force on a container wall due to perfect reflection of surface waves is (Smith, 1993):

$$F_r = \frac{1}{4}\rho g a^2 L \tag{11}$$

L is the length of the container normal to incident waves of amplitude a.

Since we do not have the information on the waves, F_r is not explicitly included in the model. However, if the waves travel in the wind direction, we could implicitly represent the wave radiation by selecting a higher value for the air drag coefficient.

Analytical Solution

To test the movement equation for a container, we use experimental data from Cabioc'h and Aoustin (1997). To simplify the drift analytical calculus, the Coriolis factor (f) has been neglected. At mean latitude 48.5° (in this study), f is equal to 1×10^{-4} s^{-1}. Others terms of Eq. (8), respectively F_a and F_w, are of the order of O[10^2 kg m s^{-2}]. We show that our analytical result fits well with their experimental drift.

The immersion ratio is a key parameter that is usually unknown in actual situation.

The immersion ratio can be expressed as:

$$I = 100\frac{S_w}{S_a + S_w} \ (\text{in}\%) \tag{12}$$

With the assumption of a steady state and neglecting Coriolis parameter, Eq. (8) can be written as:

$$\rho_a C_a S_a |\vec{V}_a - \vec{V}|(\vec{V}_a - \vec{V}) + \rho_w C_w S_w |\vec{V}_w - \vec{V}|(\vec{V}_w - \vec{V}) = 0 \tag{13}$$

Combining (12) and (13) leads to:

$$\rho_a C_a (100 - I)|\vec{V}_a - \vec{V}|(\vec{V}_a - \vec{V}) + \rho_w C_w I |\vec{V}_w - \vec{V}|(\vec{V}_w - \vec{V}) = 0 \tag{14}$$

Since $C_a = C_w = 1.0$, with the assumption of a null water current, we get:

$$(100 - I)|\vec{V}_a - \vec{V}|(\vec{V}_a - \vec{V}) - rI\vec{V}|\vec{V}| = 0 \tag{15}$$

with $r = \rho_w/\rho_a$.

The solution is:

$$V = V_a \frac{100 - I - \sqrt{rI(100 - I)}}{100 - (1 + r)I} \tag{16}$$

Figure 2 displays Eq. (16) with respect to the immersion ratio and with

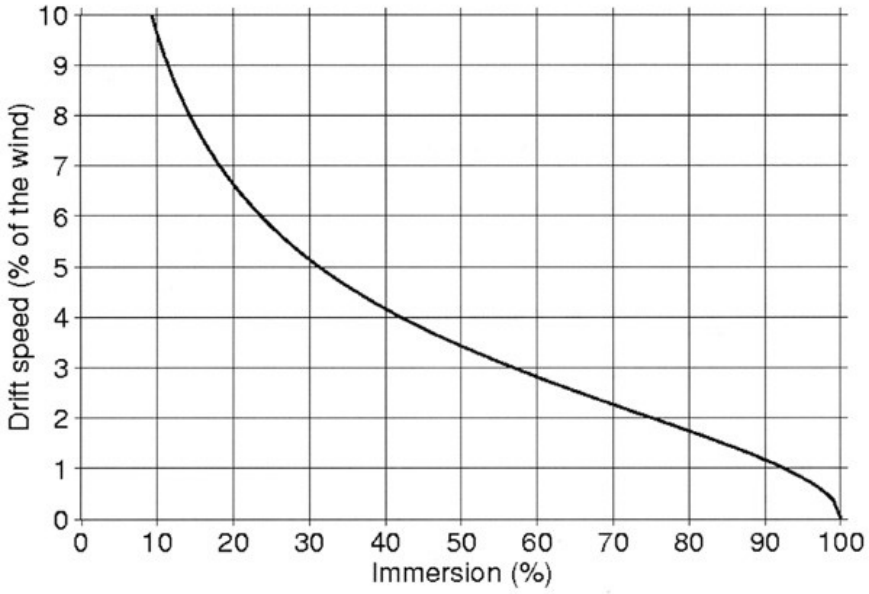

Fig. 2 Calculated drift (Jan, 1996).

$$r = \frac{\rho_w}{\rho_a} = \frac{1026}{1.29} \cong 795$$

The solution of Eq. (16) fits the experimental plot of Cabioc'h and Aoustin (1997). It is found that the container speed is very sensitive to the immersion ratio *I*. In the numerical models presented in Discussion, the Coriolis parameter is taken into account for the container drift.

If a container is moved on to land, then that container is considered beached and takes no further part in the simulation.

Atmospheric forcing

The atmospheric forcing was provided by the winds and sea level pressure forecasts from a global atmospheric model. This primitive equations atmospheric model is the European Centre for medium-range weather forecasts (ECMWF) model. The ECMWF horizontal grid mesh model is regular and of the order of $1° \times 1°$. We used atmospheric data from model analyses (i.e. forecast output plus data assimilation process). We mention that errors on our forcing fields are those commonly made in models. Briefly, an analysis is composed first by a numerical forecast. Then, models' error is related to the physics of the model and numerical bias. Analysis is also composed by a data assimilation cycle that integrates a large number of observations. Errors come from measurements because data are from multiple origins (buoys, ships, satellites, radiosondes observations...). Moreover, the spatial and temporal distribution data is irregular. For some areas, number of observations is very large (North America, Europe) but for some other, it is a desert for observations (ocean).

An analysis is a complex process to obtain a 3D representation of the atmosphere. To improve the analysis, a 4D variational method is used in the atmospheric model to give to the model, at initial time, a rough sketch of the atmosphere state, as realistic as possible.

Numerical simulations

The model is compared to few well-documented container losses (Sherbro, 1993; Churruca, 1996; & Tank containers, 1997) and to an in situ experiment (Dourvarc'h, 1991).

The Sherbro accident

Sherbro case is certainly one of the largest container losses in the history. During a severe storm in the Channel, at 23h30 on December 8th 1993, containership Sherbro lost 88 containers of 6.1–12.2 m lengths. Ten of them contained dangerous products such as pesticides. Only one of the dangerous containers was recovered.

Their level of immersion were unknown at the impact time, so we carried out a simulation with a several containers at different immersions. Nine simulated containers were started their drift at the accident point. Their immersion varied from 10% to 90%. Each figure on maps is related to the container immersion (container number 4 is 40% immersed). The wind analysis was provided by the ECMWF atmospheric model over the drift area (Fig. 3).

Nine simulated trajectories were compared with observations. On December 9 at 13:50, an overflight

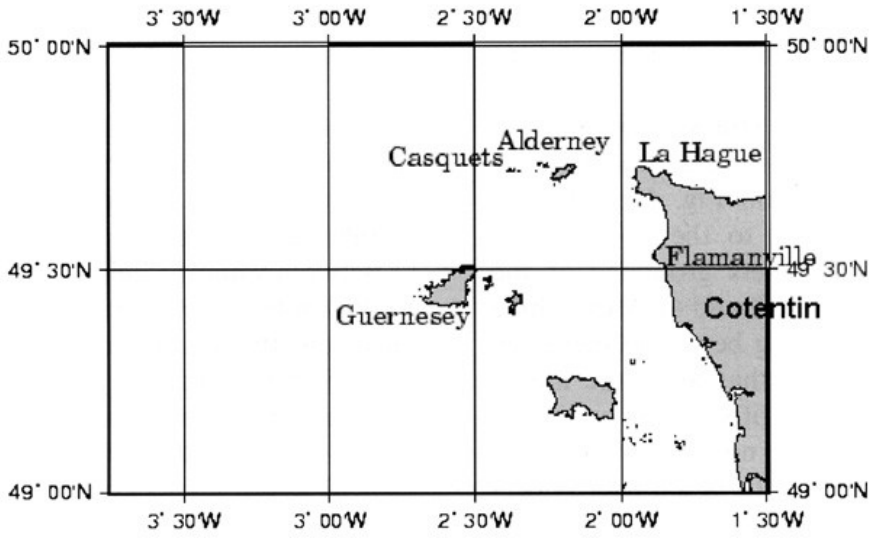

Fig. 3 Map of the drift area.

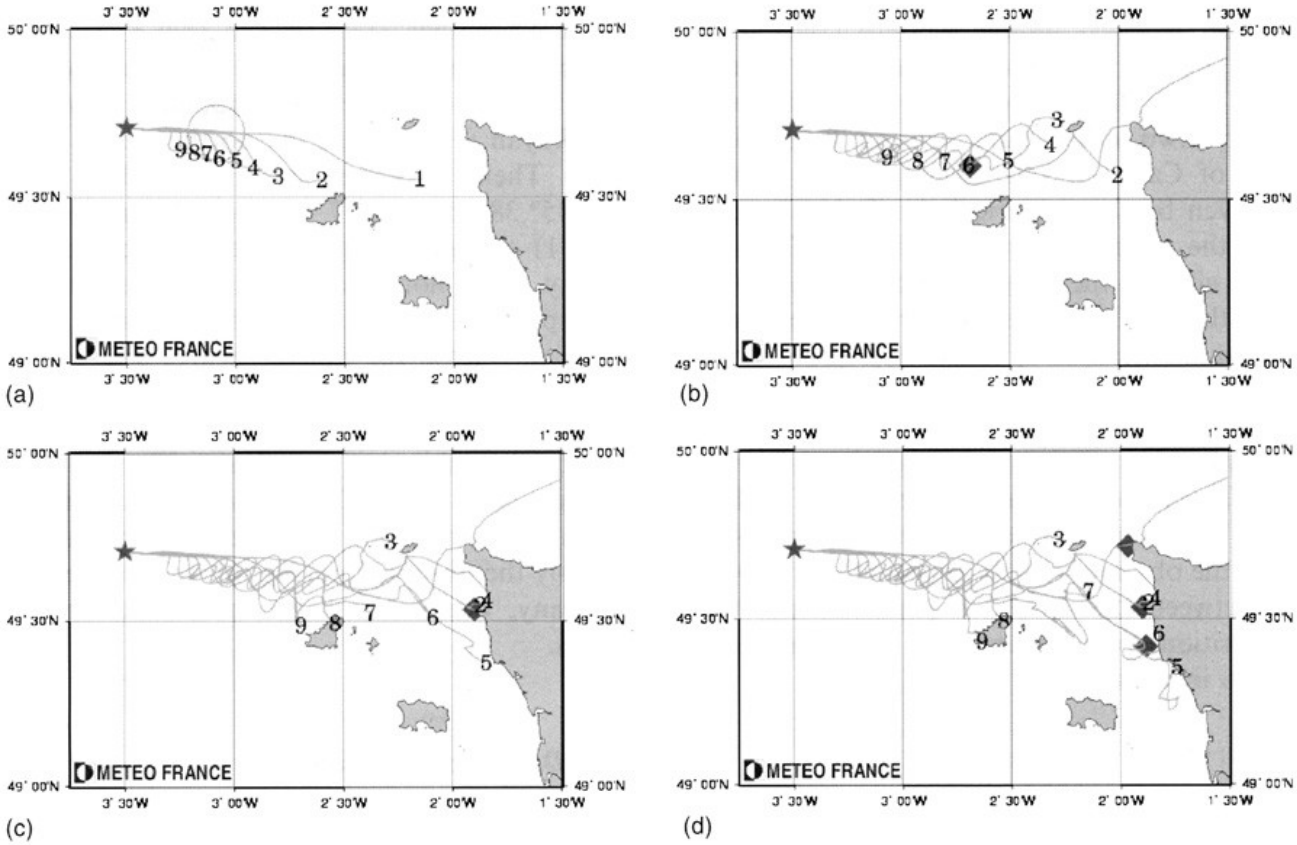

Fig. 4 (a) Sherbro. December 9, 1993 at 13:50 UTC. The container loss area is illustrated by a star. The circle represents the observed position of the containers. The trajectories simulated by the model are in grey and the positions of the nine containers in black. Container numbers correspond to their degree of immersion (time 10%). (b) Sherbro. December 10, 1993 at 12:00 UTC. The container loss area is illustrated by a star. The square represents the observed position of the containers. The trajectories simulated by the model are in grey and the positions of the nine containers in black. Container numbers correspond to their degree of immersion (time 10%). (c) Sherbro. December 11, 1993 at 12:00 UTC. The container loss area is illustrated by a star. The square represents the observed position of the containers. The trajectories simulated by the model are in grey and the positions of the nine containers in black. Container numbers correspond to their degree of immersion (time 10%). (d) Sherbro. December 12, 1993 at 13:30 UTC. The container loss area is illustrated by a star. The squares represent the observed position of the containers. The trajectories simulated by the model are in grey and the positions of the nine containers in black. Container numbers correspond to their degree of immersion (time 10%).

spotted 20 containers within a large area indicated by the circle on Fig. 4a. Immersion ratio was not easy to determine from the overflight but can be estimated from 40% to 80%. Notice that almost all of the calculated trajectories cross this zone. The numerical results best fit the observations were for immersion fractions ranging between 60% and 70%.

On December 10, seven containers were drifting fourteen miles south west of Casquets area (square on Fig. 4b) with a same kind of immersion ratio than

the previous observations. The model forecast fits exactly this observation for a 60% submerged containers.

On December 11, wind was still strong and one container full of cigarettes was found beached near Flamanville city coast (square on Fig. 4c). Our numerical results were very close to the observations showing two simulated containers grounded at the coast near Flamanville (numbers 2 and 4). More, three observed containers were drifting between Guernesey and the Cotentin coastline. In that area, the model simulates also three containers drifts corresponding to the immersions of 50–60%. We notice that the 30% immersed container is predicted to beach near Alderney Island.

On December 12, 13:30 pm, a pesticides container was recovered. At 17:30, an air overflight succeeded in locating seven containers (squares on Fig. 4d). Three of them beached on the western coast near Flamanville. Two containers were drifting in the surroundings of La Hague Cape and one of those was damaged. The two other were drifting four miles North West of Carteret. The mean position of the containers given by the numerical simulation is consistent with the observations. Nonetheless, for immersion ratio close to the extreme percents ranges (10 and greater than 80%), simulated trajectories were too fast (container number 1) or too slow (numbers 8 and 9). Containers 8 and 9, 80% and 90% immersed are beached on the North coast of Guernsey Island (Fig. 4d) and that was not observed.Container 1 drifted too far in the Northeast direction. The hypothesis of 10% immersed container is unrealistic according to the observations. It appears that the best agreement between the simulated positions and the observed positions were given by the containers having a 60% immersion.

The Churruca container incident

The ship Churruca lost a tank-container, in the entrance of the Channel on February 7, 1996 during stormy conditions. This container was first observed two days later, and a second time when it reached the coast close to Perros–Guirec, after a more than five days drift. The container immersion ratio (I) has been estimated to 25% which is the immersion level when the container was recovered. We conducted two distinct simulations: one with the container initial position at the time of loss and a second simulation initialised with the intermediate observed position. For each case, the model was forced by the ECMWF winds analysis. At the time of the loss on February 7, winds were about North West 50 knots decreasing 20 knots backing progressively Southwesterly on February 8.

On February 9 at 10 UTC, the container was located as shown by the squares in Fig. 5a. Winds were South West 30 knots. This position is compared with the first simulation. The best fit with the observed position was for 50–70% immersion ratio as shown in Fig. 5a. But the observed position is north to the simulated position.

Between 9 and 13 February, winds were Westerly 20 to 40 knots. On February 13, the container was beached on the coast near Perros–Guirec (Fig. 5b). Container ran aground in the area were the Churruca container was found. Fig. 5b shows a final position at 20–30% immersed container, which corresponds the 25% observed immersion ratio.

Containers lost in December 1997

On December 31st, 1997, a ship lost several containers off La Coruna (Spain). On January 21st 1998, two floating containers were found, drifting 150 NM off Royan (France), in the northern area of Biscaye Bay. Their positions were reported at 11:00 am (by 45° 38′2 N –3°51′7 W) and 3:35 pm (by 45° 39′5–3°54′1) the same day. These tank containers were empty, but not cleaned, and were dedicated to transport of a blend of gasoline additive, known to be highly toxic for human beings and for environment (MARPOL A classification, IMDG class 6.1). The tank container come in an open rectangular box standard to shipping containers ($20 \times 8 \times 8$ ft). Simulation with the ECMWF winds (about 13 knots from SE) shows that a container 60% immersed fits exactly the observation (Fig. 6). In this area, south of Brittany, tide currents are small and no tide loop exists.

The Dourvarc'h experiment

Experiments on drifting at sea were carried out in 1991 and 1992, off the coasts of Brittany. They were conducted by CEDRE, involving IFREMER and the French Navy.

A 20 ft (6.1 m long) container that emerges 0.7 m from water was instrumented with a wind recorder and a GPS positioning system with real time transmission to a ship (Fig. 7). The dimensions of this type of container are $6.1 \times 2.43 \times 2.43$ m. During the experiment, the container immersion ratio was 70%. GPS positions were recorded every hour with a maximum error of 100 m. The wind recorder was composed of a wind vane, an anemometer, a compass with digital display and an acquisition recorder (Orca type). Compass deviation due to the metal mass of the container were evaluated and corrections were made.

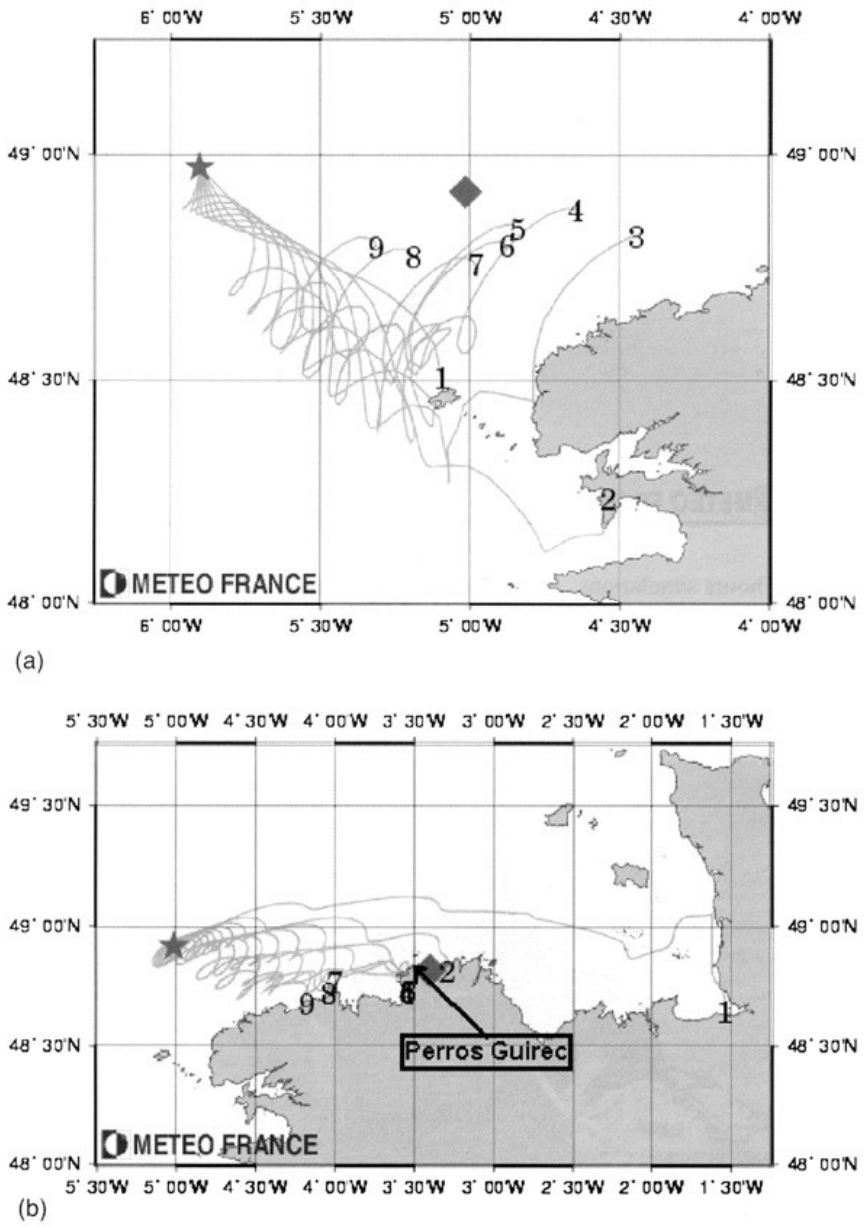

Fig. 5 (a) Churruca. Two days simulations from the initial loss starting on February 7, 1996 at 9:50 UTC. The container loss area is illustrated by a star. The square indicates the observed position of the container on February 9, 1996 at 10 UTC. The trajectories simulated by the model are in grey and the positions of the nine containers in black. The different trajectories correspond to different immersion ratios labelled in 10% (1 correspond to 10%, etc.). (b) Churruca. Four days simulations from the intermediate position starting on February 9, 1996 at 10 UTC. The container loss area is illustrated by a star. The square indicates the observed position of the container on February 13, 1996 at 6:35 UTC. The trajectories simulated by the model are in grey and the positions of the nine containers in black. The different trajectories correspond to different immersion ratios labelled in 10% (1 correspond to 10%, etc.).

The sensors were at 2 m above the sea surface. Wind measurements were averaged over 3 min every 15 min. Current measurements were recorded every 10 min with buoys at the surface and at 25 m depth. For the time of the study, current and wind data were not available. But if the numerical results fit well the drift data, then we could be confident in the ocean and container's model.

An experimental zone was delimited by the Navy. On the one occasion, the container came out off the experimental zone, it was towed back to the delimited area. This is why there were two phases. We forced the model with ECMWF winds analysis.

In both phases, the observed position of the container was east of the simulated positions (Fig. 8). During the first period, regarding the observed position, the closest simulated container is the one with 30% immersion and not 70% as it was supposed to be in reality. This could be explained by the difference between the winds fields issued from ECMWF atmospheric model (Southern sector) and the actual winds (SSW direction). Because the agreement between modelled and actual winds was much better during the second experimentation period, the closest container is 50% immersed which is more realistic compared to the 70% presupposed.

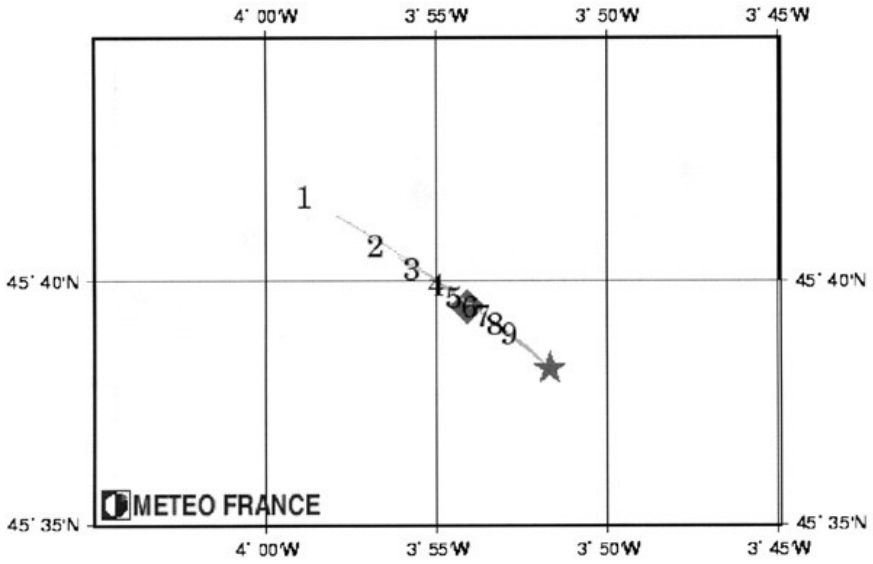

Fig. 6 Tank container. Four and a half hours simulations. A star indicates the initial position on January 21st 1998 at 11 UTC. The square figures the observed position of the container on January 21st 1998 at 15:35 UTC. The trajectories simulated by the model are in grey and the positions of the nine containers in black. Container numbers correspond to their degree of immersion (time 10%).

Fig. 7 Dourvarc'h experiment.

Discussion

Drift studies of objects lost in the sea are often empirical. We have proposed a numerical solution based on a simple mechanical concept to resolve the non-linear processes that affect the containers' trajectory. These results demonstrate good accuracy between simulated drifts and observations.

The Churruca drift study is a representative case because it illustrates that ECMWF winds are too strong and too Southeast leading to a position of container 2 far away from the observed (Fig. 5b). During the second drift period, the ECMWF wind analysis give a container's position to the right place and with a good percent of immersion (20% from simulation, 25%, the immersed ratio observed).

The role of the wind is crucial for ocean surface drift prediction model. Compared results under two different atmospheric models winds fields, demonstrate the realism of the ocean drift model forced by winds predictions. We have to keep in mind the error made on the wind vector analysis. This affects the dynamic moment applied at the surface of the ocean. Because we were searching for the forcing data that give the more realistic final position of containers, we used available wind fields.

Our simulations are performed for progressive immersed ratio every ten percents. A refined range of immersion in a quantitative study would reduce the containers' research area. But on an operational point of view, this value is difficult to get precisely, as far as calculations allow rough estimation of the buoyancy.

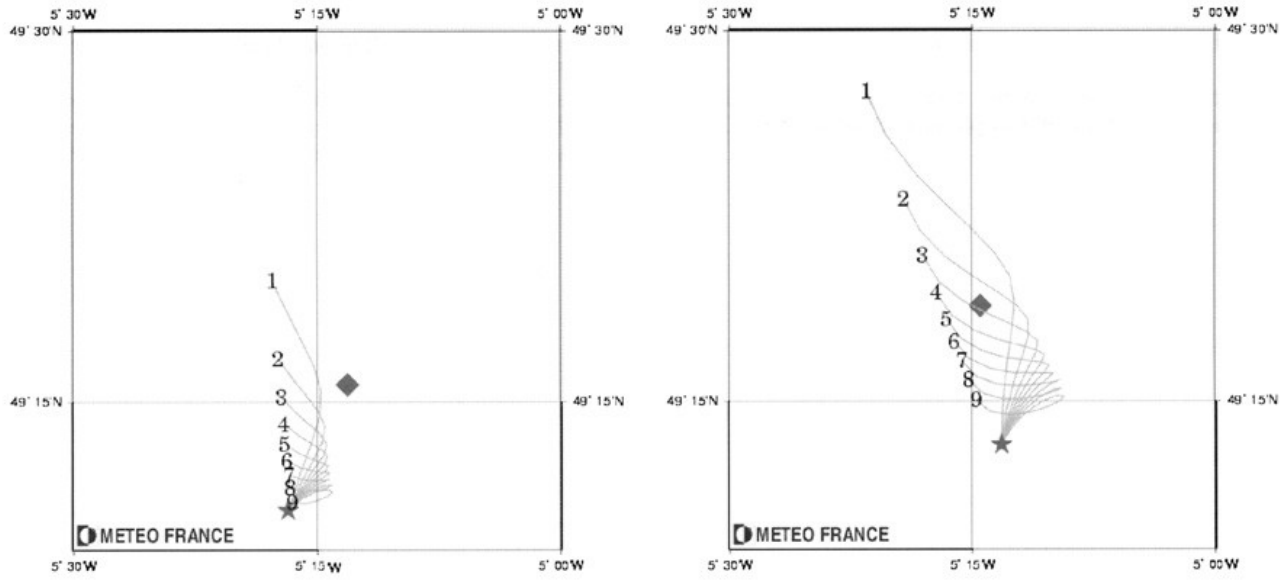

Fig. 8 Dourvarc'h. (a) Phase 1: April 9, 1991. 8 h simulation starting at 11 UTC. (b) Phase 2: 11 h simulation starting at 22 UTC. A star indicates the initial position. The square figures the observed position of the container. The trajectories simulated by the model are in grey and the positions of the nine containers in black. Container numbers correspond to their degree of immersion (time 10%).

In case of accidental marine pollution, Meteo-France provides assistance to the marine pollution emergency response operations authorities. Meteo-France can act at a national level within the response plan POLMAR-MER in case of a threat for the French coastline, and at an international level within the Marine Pollution Emergency Response Support System (MPERSS) for the high seas. The model is available to be run on the forecast period required by the alert message (typically 48 h). This system enables an investigation of a forecast scenario to be made in real time. Since March 1998, we had about two real time operations, each year. But for those cases the container sunk or was lost. The system can be used also for other kind of floating bodies and was used with success for buoys and one capsized ship (Vaysse, 2000).

Perspectives

Our study has found that results are sensitive to the mixed drag coefficient Cd (Eqs. (9) and (10)). A study has shown the effect of the Cd value on the containers' paths (Jan, personal communication, 1996). A pertinent Cd will enhance proportionally the parameterisation of the forces applied on the container. A future step in further development of the model will be a study on the sensitivity of containers' drift to the drag coefficients (C_a and C_w).

Moreover, studies on the impact of waves radiation force on the sea ice drift have shown that it could be nearly double the wind force (Perrie and Hu, 1997; Smith, 1993). The wave force is already taken into account in the air drag coefficient and could be best fitted regarding to the results of a sensitivity study, as mentioned above.

We also note the sensitivity of the container trajectories to the immersion ratio which is a parameter difficult to estimate in operational cases.

Acknowledgements—This work has been performed during the graduate visit of G. Jan, Y. Landau and E. Loiseau to DPrévi/MAR. Illustrations are kindly provided by CEDRE. All the plots are made with the Generic Mapping Tools GMT version 3.

References

Bigg, G., Wadley, M., Stevens, D., Johnson, J., 1996. Prediction of iceberg trajectories for the North Atlantic and Artic Oceans. Geophysical Research Letters 23 (24), 3587–3590.

Cabioc'h, F., Aoustin, Y., 1997. Criteria for decision making regarding response to accidentally spilled chemicals in packaged form: hydrodynamic aspects. Spill Science and Technology Bulletin 4 (1), 7–15.

Crépon, M., Houssais, M., Saint Guily, B., 1988. The drift of icebergs under wind action. Journal of Geophysical Research 93 (C4), 3608–3612.

Daniel, P., 1996. Operational forecasting of oil spill drift at METEO-FRANCE. Spill Science and Technology Bulletin 3 (1/2), 53–64.

Daniel, P., Poitevin, J., Tiercelin, C., Marchand, M., 1998. Forecasting accidental marine pollution drift: the French operational plan, Oil and Hydrocarbon Spills, Modeling, Analysis and Control. Computational Mechanics Publications, 43–52.

Jan, G., 1996. Adaptation du modèle de dérive de nappes d'hydrocarbures de Météo-France à la dérive de conteneurs perdus en mer, Mémoire de DEA, Université de Liège, p. 36.

Madsen, O.S., 1977. A realistic model of the wind-induced Ekman boundary layer. Journal of Physical Oceanography 7, 248–255.

Perrie, W., Hu, Y., 1997. Air–ice–ocean momentum exchange. Part II: Ice drift. Journal of Physical Oceanography 27, 1976–1996.

Poon, Y.K., Madsen, O.S., 1991. A two layers wind-driven coastal circulation model. Journal of Geophysical Research 96 (C2), 2535–2548.

Smith, S., 1993. Hindcasting iceberg drift using current profiles and winds. Cold Regions Sciences and Technology 22, 33–45.

Vaysse, F., 2000. L'épopée de Navifax-direct. Metmar (186), 3–7.

Wu, J., 1982. Wind-stress coefficients over sea surface from breeze to hurricane. Journal of Geophysical Research 87, 9704–9706.